# Assessing Corn Yield and Nitrogen Uptake Variability with Digitized Aerial Infrared Photographs*

M.D. Tomer, J.L. Anderson, and J.A. Lamb

## Abstract

*Methods for large-scale mapping of crop variability are needed for precision farming applications. We hypothesized that aerial-infrared photographs can predict corn yield and N uptake variability. A 2.6-ha area in Minnesota was cropped with corn in 1991 and 1992. Photographs of bare soil and of the mature crops were color scanned. Corn yield and N uptake were determined at 58 locations, and were related to phototone data using multiple regression. Spatial analysis of imagery showed that the crop canopy was more influenced by soil conditions in 1991 than in 1992. This is attributed to the cooler climate in 1992. Consequently, harvest data were better predicted in 1991 than in 1992. In 1991, 65 percent of yield and 59 percent of N-uptake variability were captured by phototones; respective values for 1992 data were 47 percent and 37 percent. Use of aerial photographs for spatial modeling of crop growth can work, but multi-year studies are recommended.*

## Introduction

In conventional agriculture, crop management decisions are generally based on the productive history of each individual field. An alternative strategy is to base management practices on the productive capacities of individual soil types within fields. This strategy, known as precision agriculture, has the potential to improve farm profitability and minimize adverse effects of agriculture on the environment. Precision agriculture can be implemented using variable-rate technology (VRT). VRT provides the ability to vary fertilizer rates, pesticide applications, and tillage operations across fields. For example, fertilizer amendments can be reduced on soils with low productivity, or with a high potential for leaching or runoff. However, wide use of VRT will require proof of profitability and environmental benefits. Lack of an effective mapping technique to consistently estimate spatial differences in soil productivity across the landscape is a major hindrance to the adoption of VRT (Sawyer, 1994). Conventional soil maps (based on second-order surveys) are scaled at 1:12,000 to 1:24,000, and do not have the accuracy or detail required for site-specific management, which requires scales from 1:2,000 to 1:10,000. Methods to map and delineate management areas within fields are needed to optimize application rates and quantify benefits of soil-specific management.

Large-scale aerial photographs can assist in field-scale soil mapping (Harrison *et al.*, 1987; Kunze and Lemme, 1986). Aerial photographs have been used in soil survey for many years; visual interpretation of panchromatic, color, or color infrared photographs has been used to determine locations of sampling sites and map-unit boundaries (see Campbell (1987) for an overview). Soil erosional features (Lyon *et al.*, 1986) and soil erodibility (Stephens *et al.*, 1985) have been mapped using aerial photos. Although past use of aerial photographs in crop and soil studies usually involved manual interpretation, computer digitization and spatial registration now allow statistical approaches that can quantify the variability captured with photographs. Schmidt *et al.* (1987) and Zheng and Schreier (1988) have suggested that specific soil properties (such as surface organic matter) can be mapped with reasonable confidence using aerial photographs. Everitt *et al.* (1987) showed that buffelgrass (*Cenchrus ciliaris*) biomass was correlated with red photometric reflectance, and Tucker (1979) showed that blue grama (*Bouteloua gracilis*) biomass was correlated with red and infrared photometric reflectance. Therefore, aerial photographs are helpful in assessing spatial variability in water availability and crop growth. Long *et al.* (1989) showed that yield patterns can be discerned using aerial photographs of bare and cropped surfaces. Milfred and Kiefer (1976) determined landscape patterns in loess thickness with sequential aerial photographs taken during crop maturation. In both these cases (Long *et al.*, 1989; Milfred and Kiefer, 1976), photographs taken at physiological maturity of the crop were the best for showing patterns of differentiation in the crop canopy within uniformly managed fields. Photographs of a developing crop can be used to discern management effects, but soil landscape effects on the crop are best discerned at maturity.

There are two likely mechanisms that will allow crop and soil mapping using aerial photographs. First, growing vegetation absorbs red light (0.6- to 0.7-μm wavelengths), and reflects near infrared light (0.7- to 1.3-μm wavelengths). Plant stress and maturation are accompanied by greater reflectance of red light and more absorption of infrared light (Collins, 1978). A loss of growth and vigor in the crop can therefore be detected by increased red reflectance and lowered infrared reflectance. Monitoring drought stress by satellite imagery has been based on this principle (Campbell, 1987). Similarly, differential crop maturation within fields might also be captured by properly timed color-infrared photographs. If so, the hy-

---

---

Department of Soil Science, University of Minnesota, St. Paul, MN 55108.

M.D. Tomer is presently with the New Zealand Forest Research Institute, Private Bag 3020, Rotorua, New Zealand.
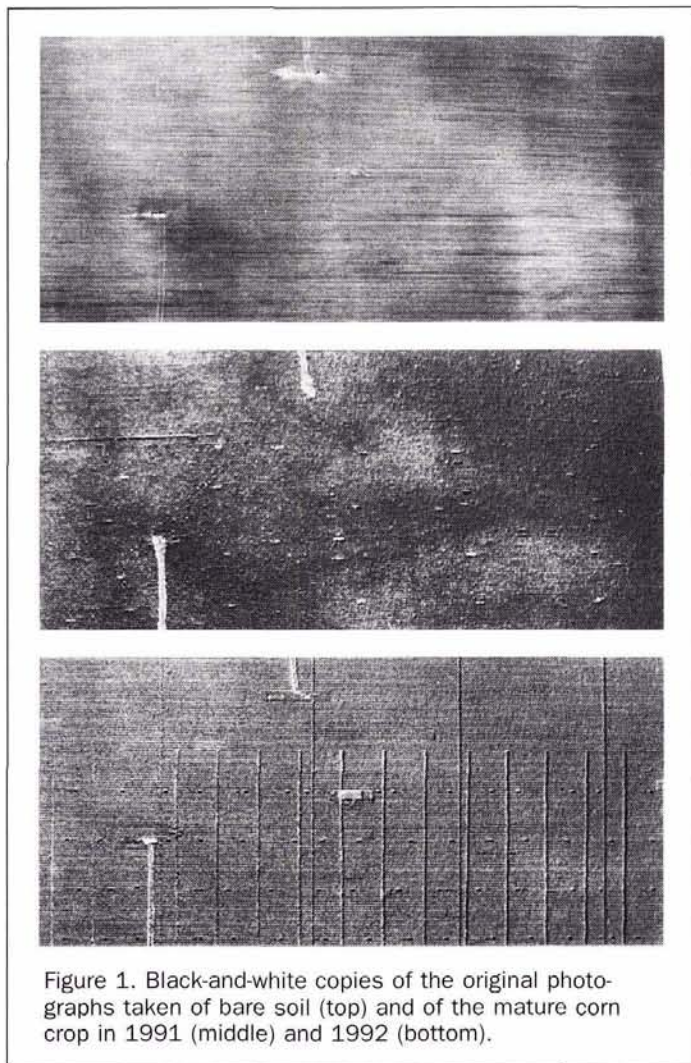
---

Figure 1. Black-and-white copies of the original photographs taken of bare soil (top) and of the mature corn crop in 1991 (middle) and 1992 (bottom).

red color photographs can be used to predict and map variation of corn grain yield and nitrogen (N) uptake within a uniformly managed field. The second objective was to compare the predictive capacities of photographic data with that of topographic data and geostatistical methods. An important aspect of this work was to ensure that observed spatial patterns in crop growth were consistent with distributions of soils and soil water availability. Soil-water storage was therefore monitored along a transect of access tubes to provide a basis for comparison between soil water and crop growth.

## Methods

The study was conducted at the Northern Cornbelt Sandplains Management System Evaluation Area, a water-quality research site on the Anoka Sand Plain in east-central Minnesota (Sherburne County). A detailed description of the site is provided by Delin et al. (1994). The dominant soil is the Zimmerman fine sand, classified as a mixed, frigid, Argic Udipsamment (Soil Survey Staff, 1992). Aerial-infrared photographs of the continuous corn research area (dimensions of 236 by 109 m) were acquired at crop maturity in 1991 (29 August) and 1992 (26 August), and of bare soil (post-seeding conditions) in 1992 (18 May). Flights were at an approximate altitude of 250 m above the surface, at an approximate ground speed of 200 km/h. A 35-mm format camera (Minolta X700[1]) with a 28-mm Minolta all glass lens and yellow filter (Wratten #15) was used. Echtachrome infrared (ASA 100) film was used at a 200 ASA setting. Exposure time was 1/500 second, with a 5.6 F-stop setting. These settings were based on the experience of the photographer we contracted; use of a fixed aperture and a variable shutter speed at a higher ASA setting was used to limit exposure in the visible range and allow greater sensitivity in the infrared range. For each photographic date, a separate roll of film was used and developed immediately using the same developing facility. The three rolls all came from the same film batch, and film was stored at $-23°C$ to ensure minimal degradation in film sensitivity during the study.[2]

An elevation survey of this area was performed using a Geodimeter (Model 136 theodolite), at an average grid spacing of 4.5 m. Survey results were imported as a point map coverage into ARC/INFO (ESRI, 1992), and a raster digital elevation model (DEM) of 2-m cell size was interpolated using a universal kriging program. The elevation model was exported to KHOROS (KHOROS, 1991) for slope calculations (steepness and direction of slope). The slope maps were calculated using 4-m cells (alternate rows and columns were extracted from the image) to reduce effects of local interpolation errors and microtopography.

Black-and-white copies of the original aerial photographs are shown in Figure 1. The photos were scanned with a Howtek Scanmaster three-color scanner at 150 dpi resolution, to give eight-bit (256 levels), three-band (RGB) tagged image file format (TIFF) images. The scanner measured relative intensity of light reflected from the photographs after passing filters that allow transmission of red, green, and blue wavelengths. Red, green, and blue image bands indicate photographic halftones within infrared, red, and green bands, respectively. Greater halftone values indicate greater reflectance in that band. In this paper we abbreviate the term "photographic halftone" to "phototone" to denote image data obtained by digitizing photographs. Implicitly, the process of

pothesis that patterns of crop maturation are due to soil variability would need to be verified in the face of alternative explanations. Spatial patterns across crop canopies have also been related to inconsistencies in field operations (Baber, 1982) and disease (Gerten and Wiese, 1987).

The second mechanism involves color differentiation in surface soils (e.g., darker soils generally have greater organic matter and/or water content). Near-infrared reflectance decreases with higher organic matter (Frazier and Cheng, 1989). Stoner and Baumgardner (1981) showed that reflectance spectra of soils are influenced or dominated by organic matter, which affects water and nutrient availability. Because surface organic matter levels may also indicate relative erosion severity, or areas of greater water availability to plants (e.g., lowland areas), photometric reflectance of bare soil may be helpful in mapping soil conditions that affect plant growth.

Maturity stage, leaf area and orientation, shadow, soil reflectance, solar zenith angle, and surface topography (aspect and slope) all influence reflectance characteristics of plant canopies (Colwell, 1974). These factors may not entirely complicate map prediction of crop growth, because most are also influenced by yield determinants such as plant population and canopy height and density. Therefore, aerial photographs provide a possible tool to produce maps describing crop growth variation within fields for applications in soil-specific management. The primary objective of this research was to determine if data obtained from scanned aerial-infra-

photograph acquisition, film processing, and digitization is an analog to digital data conversion. This means that phototone values are relative and best interpreted in terms of variability observed within each image, as emphasized in this paper. Comparison of absolute phototone values between images would require calibration by placing ground reference targets of known reflectance values at the survey site.

Of the three photographs, the 1992 crop image showed the least camera angle distortion (most uniform measures of length and width of the cropped area across the photo). The bare soil and 1991 crop images were registered to match pixel locations on the 1992 crop image using common features (corners of the cropped area and monitoring wells) visible on each pair of photos and a tiepoint matching and image warping program (VWARP) in KHOROS (KHOROS, 1991). The VWARP program aligned "source" images (bare soil, 1991 crop) to the "target" image (1992 crop), and calculated new source images by bilinear interpolation. The three images were then clipped to delete non-cropped land surrounding the area. These images were 453 rows by 955 columns (about four image cells per metre). Image coordinates of corners of the cropped area, and of three monitoring wells within the cropped area, matched ground-survey coordinates to within 1 m.

A disadvantage of the high photographic resolution was the distinction between the crop and shadow (within crop rows) that dominated crop images. These distinctions were minimized by a low-pass filter applied to a window eleven by eleven pixels in size. This provided spatial averaging across 2.7 metres (three crop rows) to minimize intra-row variation in the crop images. Every eighth pixel was then extracted from the filtered image to create an image with the same dimensions (56 rows, 119 columns) as the DEM for the area. The final map products were nine layers representing infrared, red, and green phototones for the bare soil and crop maturity (1991 and 1992) images, plus elevation, slope, and aspect maps of the area. These maps were converted to ASCII format for import to PC-based spreadsheet (Microsoft, 1992) and geographic information system (LMIC, 1990) software.

Each photographic image was summarized for spatial autocorrelation. We believed a separate spatial analysis for each band would be redundant, and so calculated a composite image for each photograph using principal components analysis. One thousand data points (a 15 percent sample) were randomly selected from the images (omitting the three rows and columns at image edges). A principal component (PC) analysis of the three bands for each image was performed using the PRINCE procedure of SAS (SAS Institute, 1988). The first PC for each of the three images was calculated; and the correlograms and variograms were then determined for each of these images (see appendix for a brief on statistical terminology).

The crop was harvested at 58 sampling locations discernible on the photographs. Yield was determined from grain harvested along 12.2 m of row (6.1 m from each of two rows), and corrected to a constant grain moisture of 15.5 percent. Above-ground biomass samples (from 1.5 m of row) were also taken at each sample location. Nitrogen concentrations were determined by Kjeldahl digestion on samples of grain, cob, and stover (Nelson and Sommers, 1973), expressed on a kg/ha basis, and summed to give total N uptake. Nitrogen fertilizer applications included 22 kg N/ha at planting in both years and split applications of 56 and 78 kg N/ha in 1991, and 78 and 67 kg N/ha in 1992.

The high resolution of the photos and scanned images provided the advantage of precise spatial registration. Alleys (which marked harvest plots in 1992) and corn rows were visible in the original photographs (Figure 1) and scanned images, and were used to determine the row and column coordinates of each harvest location. Phototone and topo-graphic data corresponding to these harvest locations were extracted from the processed imagery.

Extracted image data (both photographic and topographic) were compared to yield and N uptake data. Regressions were performed using grain yield and total N uptake data (1991 and 1992) as dependent variables, and using individual phototone bands (infrared, red, green) from the bare soil and appropriate crop cover (1991 or 1992) as independent variables. Separate regressions between harvest and topographic data included a quadratic term for aspect (to allow for a possible minima near a southerly exposure), and interaction terms for the independent topographic parameters. Stepwise- and backward-model-selection methods were applied using the REG (regression) procedure of SAS (SAS Institute, 1988), using a $p = 0.1$ as the criterion for variable inclusion or deletion ($p$ value tested the hypothesis that a regression coefficient equals zero). Final model selection was based on significance of partial sums of squares, maximization of adjusted $R^2$, and consistency between models. Regression residuals were checked for trends (with both topographic and map coordinates), error correlation, and spatial autocorrelation. Variograms of grain yield and N uptake data were calculated, and jackknife kriging errors were compared to regression residuals of the selected regression models (see appendix for a brief on statistical terminology).

Soil and soil-water data were collected from 12 neutron probe access tubes installed along the length of the cropped area, 9 m (ten crop rows) from its southern edge. Soil water monitoring was performed on 25 dates during the 1992 growing season with a neutron probe (access tubes were not installed in 1991). Measurement depths were at 10-cm intervals between 0.3 and 1.6 m. The access tubes were included in the elevation survey of the site. Profiles of cumulative soil water storage and changes in storage between measurement dates were calculated to determine changes in water storage after irrigation or rainfall, and during subsequent periods of crop-water use. There were only two time periods exceeding one week in duration with no rainfall or irrigation. These periods occurred after irrigation (2.5 cm) on 22 July (from 23 to 31 July), and after rainfall (4.4 cm) on 7 August (from 12 to 20 August)[3]. Data collected during these periods were examined for consistent patterns of water loss (to a 1.65-m depth).

## Results and Discussion

### Exploratory Analysis

The topographic map of the continuous corn area (Figure 2) shows the total relief is less than 3 metres. Lowland positions are found at the eastern edge and in the southwest quadrant of the area. A broad ridge dominates the central portion of the area between these lowland areas. Slope varies from zero to 7 percent. There are two noteworthy differences between crop-
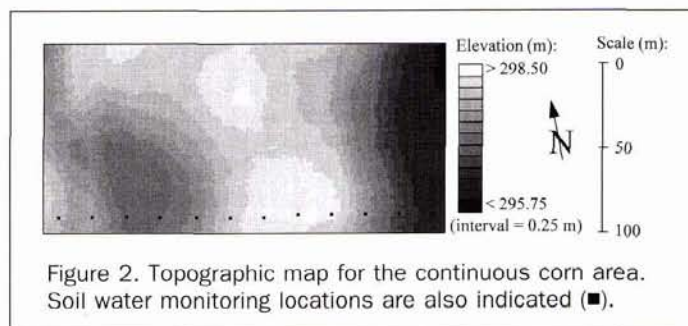


Figure 2. Topographic map for the continuous corn area. Soil water monitoring locations are also indicated (■).

---

[3]Battery failure prevented monitoring between 8 and 11 August.

years: (1) the summer months of 1992 were cooler than in 1991 (Table 1), and (2) a linear-move irrigator was installed and used in 1992, whereas the 1991 crop was rainfed. Precipitation during summer 1991 was relatively high, and approximately equal to the rainfall plus irrigation for the summer months of 1992 (Table 1). However, the temporal distribution of rainfall in 1991 did cause some crop-water stress.

Effects of the cooler growing season of 1992 include less grain yield and N uptake in 1992 relative to 1991 (Table 2). Yield is also less variable in 1992, as estimated by the coefficient of variation (10.3 percent in 1991, 7.8 percent in 1992; see Table 2). Univariate statistics of the yield and phototone data used in regression analyses (Table 2) show that the data conform with normal distributions (by Wilk's W statistic, $p = 0.05$). Topographic data (elevation, slope, and aspect) corresponding to the harvest sample locations were not consistent with normal distributions.

To examine spatial structures of the images, the first principal component of the three bands was calculated (by eigenvector weights given in Table 3) to provide a composite (gray scale) image for each coverage (Figure 3). These composite images account for 94 to 98 percent of the total vari-

ance in the band-separated data (Table 3). The degree and pattern of variability within each image may be compared by visual means, and by the correlation structure of each image (Figure 3). With both types of comparison, the greatest similarity occurs between the bare soil and 1991 crop maturity image. This implies that the crop canopy was more influenced by soil conditions in 1991 than in 1992. The difference between years is attributed to the cooler climate of 1992 and use of irrigation, which resulted in slow maturation and negligible crop stress. The similarity between the bare soil and 1991 images, and the contrast between crop images, suggests that color variation across a bare soil surface is due to factors

TABLE 1. COMPARISON OF CLIMATE DURING THE SUMMER MONTHS OF 1991 AND 1992.

| Climatic Parameter | June 1991 | June 1992 | July 1991 | July 1992 | August 1991 | August 1992 |
|---|---|---|---|---|---|---|
| Ave. Max. Temp. (°C) | 26.1 | 22.9 | 25.6 | 22.8 | 26.1 | 23.0 |
| Ave. Min. Temp. (°C) | 15.5 | 11.1 | 15.8 | 12.1 | 14.7 | 12.2 |
| Ave. Daily Temp. (°C) | 20.8 | 16.9 | 20.7 | 17.4 | 20.4 | 17.7 |
| Cumulative GDD* | 982 | 779 | 1572 | 1208 | 2150 | 1656 |
| Ave. Daily GDD | 19.3 | 13.6 | 18.9 | 13.8 | 18.6 | 14.4 |
| Total ppt. (cm) | 10.8 | 6.1 | 12.6 | 8.2 | 10.7 | 9.3 |
| Irrigation (cm) | ** | 5.1 | ** | 2.5 | ** | 2.5 |

*Monthly summation of daily average of max. and min. temperature (°F), minus 50.
**The irrigation system was not installed until spring, 1992.

TABLE 2. UNIVARIATE STATISTICS FOR VARIABLES USED IN REGRESSION MODELING. NOTATION: B = BARE SOIL IMAGE; 91 = 1991 CROP IMAGE; 92 = 1992 CROP IMAGE; I, R, G = INFRARED, RED, GREEN BANDS, RESPECTIVELY.

| Variate | Units | Mean | St. Dev. | Max. | Min. | p(N)* |
|---|---|---|---|---|---|---|
| BI | (8bit) | 97.8 | 9.64 | 115 | 71 | 0.120 |
| BR | (8bit) | 96.0 | 9.60 | 116 | 72 | 0.457 |
| BG | (8bit) | 83.9 | 8.75 | 103 | 62 | 0.339 |
| 91I | (8bit) | 103.2 | 5.23 | 118 | 91 | 0.326 |
| 91R | (8bit) | 68.8 | 8.19 | 91 | 55 | 0.100 |
| 91G | (8bit) | 68.0 | 6.41 | 84 | 56 | 0.335 |
| 92I | (8bit) | 130.2 | 5.94 | 146 | 118 | 0.787 |
| 92R | (8bit) | 77.1 | 7.05 | 100 | 62 | 0.762 |
| 92G | (8bit) | 76.2 | 7.12 | 99 | 63 | 0.337 |
| Y91** | kg/ha | 8580 | 884.4 | 10000 | 6474 | 0.056 |
| N91 | kg/ha | 137.2 | 13.4 | 161.8 | 103.7 | 0.172 |
| Y92 | kg/ha | 7072 | 554.8 | 8279.7 | 5617.2 | 0.716 |
| N92 | kg/ha | 108.2 | 11.25 | 138.8 | 88.4 | 0.430 |
| Z | m | 297.5 | 0.72 | 298.46 | 295.89 | 0.001 |
| SL | % | 2.58 | 1.52 | 6.56 | 0.19 | 0.009 |
| ASP | az | 150 | 98 | 336 | 8.5 | 0.000 |

*Normality test: Probability that Wilk's statistic would be exceeded if parent distribution is normal; **n=57 (one outlier omitted from analysis)
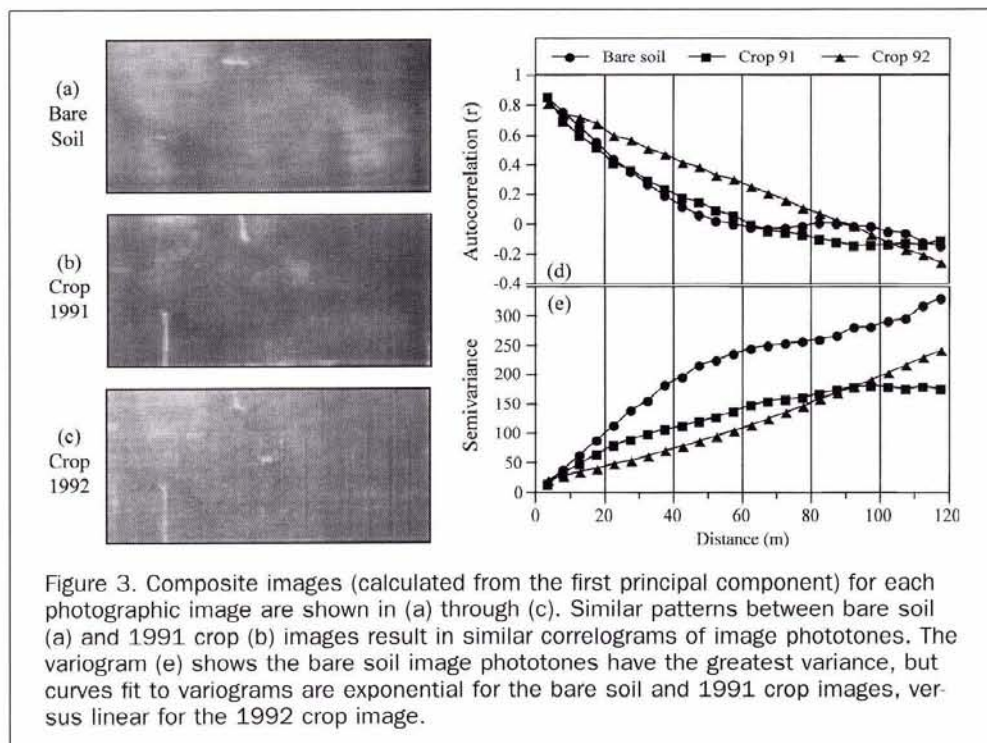Z = elevation
SL = slope
ASP = aspect



Figure 3. Composite images (calculated from the first principal component) for each photographic image are shown in (a) through (c). Similar patterns between bare soil (a) and 1991 crop (b) images result in similar correlograms of image phototones. The variogram (e) shows the bare soil image phototones have the greatest variance, but curves fit to variograms are exponential for the bare soil and 1991 crop images, versus linear for the 1992 crop image.

(e.g., organic matter) that can influence crop canopy development. Under the crop-water-stress conditions that occurred in 1991, it appears that landscape-scale differentiation in the crop canopy was associated with the distribution of soils and soil-water availability. Conversely, limited heat stress in 1992 muted spatial differentiation of the crop canopy.

## Regression Results
Regression models explain between 64 and 38 percent of the variance in grain yield and N uptake (Table 4). All terms included in the model have a $p$ value less than 0.05, except that the bare infrared (BI) term in the 1992 grain yield model had a $p$ of 0.056. The four models are consistent in the use of three terms (crop infrared and red bands, and bare soil infrared band). Coefficients are consistent (in sign) with known interactions between plant growth, soils, and light reflectance, providing a uniform basis for the models. A negative correlation between soil organic matter and near infrared light reflectance has been established by several studies (Henderson et al., 1989). Negative coefficients for the bare soil infrared band (Table 4) are therefore consistent with greater grain yield and N uptake occurring on soils with greater soil organic matter. Each model also includes terms for infrared (positive coefficient) and red (negative coefficient) crop phototone. This is consistent with the changes in light reflectance observed during plant maturation (Campbell, 1987; Collins, 1978). Differences in relative red and infrared reflectance are indicative of crop maturation patterns across the landscape. Areas of early maturation indicate greater crop stress, and less yield. Note that the magnitudes of the regression coefficients cannot be compared, due to the analog origin of the phototone data. Regression models including ratioed phototone data (infrared/red) were also examined, but explained less variance in the data than the band-separated models.

Regression models for the 1992 data have less precision (in terms of $R^2$) than do the 1991 models (Table 4). This was again due to less differentiation in the 1992 crop that resulted from the cooler conditions. A similar difference between years was observed for the regressions between harvest and topographic data. Results were significant for 1991 harvest data: elevation explained 18 percent of the 1991 yield variation, and 28 percent of the 1991 N uptake variance was accounted by elevation and slope (no interaction terms were significant). The regression coefficients were all negative and therefore consistent with the concept that less growth occurs at higher and/or steeper landscape positions. Similar regressions for the 1992 data were not statistically significant. This confirms that landscape patterns of crop growth observed in 1991 were muted in 1992. Also, on this landscape, the phototone data provide greater precision for crop mapping than do the topographic data.

## Evaluation of Regression Models
To evaluate regression models, prediction errors (actual minus predicted values) were regressed against topographic parameters (elevation and slope), and map coordinates (quadratic trend including $X$, $Y$, $XY$, $X^2$, and $Y^2$ terms). No significant relationships were found ($\alpha = 0.1$), suggesting that the regression models effectively account for the spatial trends in the data. Correlograms of model residuals and original measured data were compared (Figure 4). Correlation structure of the harvest data, which is relatively weak (i.e., autocorrelation at the closest sampling interval does not exceed 0.3; see Figure 4), is also explained by the models.

Variograms of grain yield and N uptake were fit to linear/sill variogram models, and a jackknife kriging analysis was performed. Distributions of jackknife kriging errors were compared to errors of prediction by regression (Table 5). Comparison of error distributions show that the regression has better interpolative capacity than kriging; regression errors have lower absolute mean, standard deviation, and correlation with predicted variates than kriging errors (less data
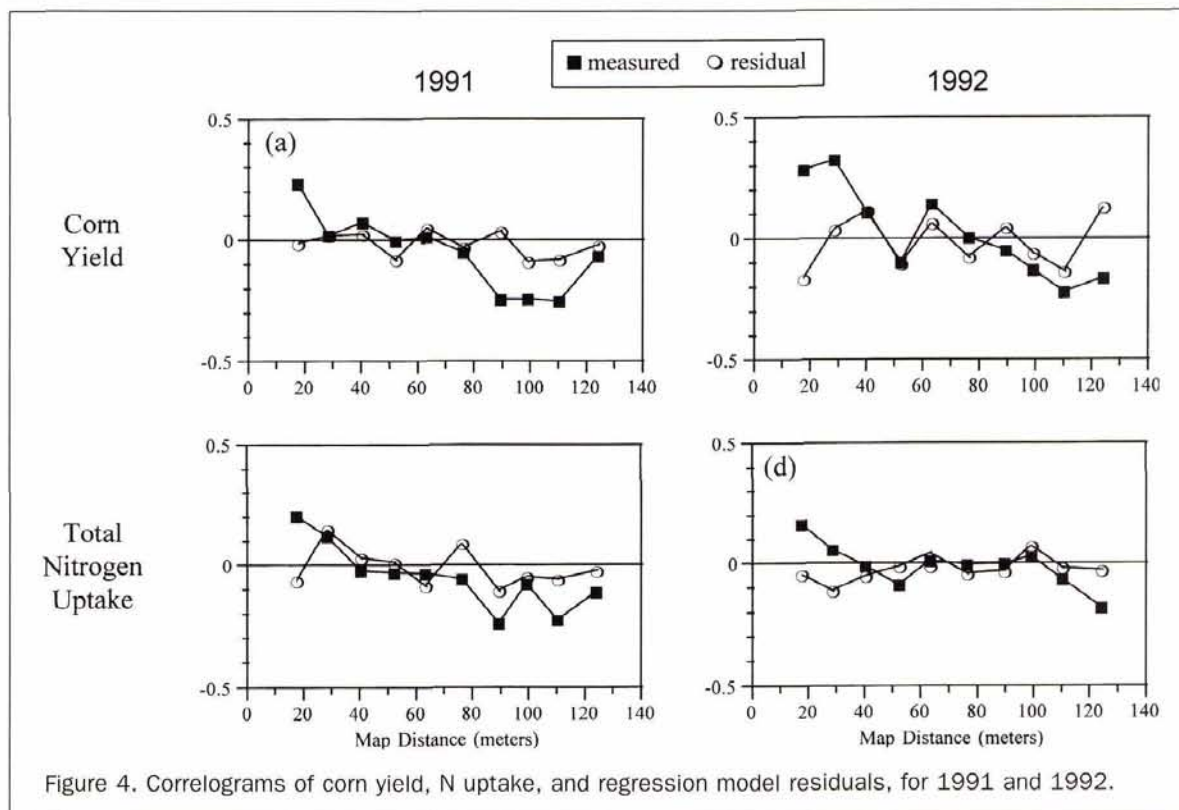


Figure 4. Correlograms of corn yield, N uptake, and regression model residuals, for 1991 and 1992.

TABLE 3. PRINCIPAL COMPONENT ANALYSIS RESULTS FOR AERIAL IMAGERY. INFRARED, RED, AND GREEN BANDS ARE DENOTED BY I, R, AND G.

| Image | % variation | Eigenvector weights | | |
| | | I | R | G |
|---|---|---|---|---|
| Bare soil | 97.7 | 0.57 | 0.58 | 0.58 |
| 1991 crop | 95.5 | 0.57 | 0.58 | 0.58 |
| 1992 crop | 94.4 | 0.56 | 0.58 | 0.59 |

TABLE 4. SUMMARY OF REGRESSION MODELS. NOTATION: B = BARE SOIL IMAGE; 91 = 1991 CROP IMAGE; 92 = 1992 CROP IMAGE; I, R, G = INFRARED, RED, GREEN BANDS, RESPECTIVELY.

| Dependent variable | Regression model | Model $R^2$ |
|---|---|---|
| **1991** | | |
| Grain Yield | $= 0.92 - 2.16*BI + 2.01*BR + 1.14*91I - 1.65*91R$ | 0.64 |
| N uptake | $= 0.97 - 1.13*BI + 0.79*BG + 0.66*91I - 1.1191R$ | 0.59 |
| **1992** | | |
| Grain Yield | $= 0.51 - 0.20*BI + 1.67*92I - 1.45*92R$ | 0.47 |
| N uptake | $= 0.43 - 0.25*BI + 1.62*92I - 1.49*92R$ | 0.38 |

TABLE 5. DISTRIBUTIONS OF REGRESSION AND KRIGING ERRORS IN PREDICTING CORN YIELD AND N UPTAKE, 1991 AND 1992. UNITS ARE KG/HA, EXCEPT FOR CORRELATIONS (WHICH ARE DIMENSIONLESS).

| | | 1991 | | 1992 | |
| | | Regression Errors | Kriging Errors | Regression Errors | Kriging Errors |
|---|---|---|---|---|---|
| Grain Yield | Mean | 0.66 | 64.01 | 0.02 | 10.14 |
| | Std. Dev. | 527.4 | 830.1 | 402.9 | 494.3 |
| | Median | 18.0 | 199.3 | −22.8 | −31.4 |
| | Skew | −0.42 | −0.46 | 0.31 | 0.79 |
| | Minimum | −1360.7 | −1806.6 | −867.2 | −958.0 |
| | Maximum | 938.6 | 1563.7 | 986.2 | 1650.1 |
| | Correlation with Yield | 0.60 | 0.89 | 0.73 | 0.83 |
| N Uptake | Mean | 0.00 | 0.46 | 0.01 | 0.48 |
| | Std. Dev. | 8.54 | 12.27 | 8.83 | 11.33 |
| | Median | −0.71 | 1.01 | −1.91 | −2.06 |
| | Skew | −0.11 | −0.36 | 0.35 | 0.68 |
| | Minimum | −19.6 | −28.9 | −19.5 | −17.0 |
| | Maximum | 17.0 | 20.8 | 21.7 | 32.3 |
| | Correlation with N uptake | 0.64 | 0.89 | 0.78 | 0.90 |

smoothing). Therefore, digitized photographs provide a better basis for interpolation than geostatistical approaches.

## Application of Regression Models

The regression equations were applied to the phototone images, using map overlay techniques, to provide maps of estimated corn grain yield and N uptake for 1991 (Figure 5) and 1992. In 1991, the smallest estimates of grain yield and N uptake are associated with the steeper slopes and upland areas, while the greatest estimates are associated with lower landscape positions; these patterns are most evident by comparing the 1991 maps (Figure 5) with the topography (Figure 2). Similar patterns of crop growth across the landscape have been reported previously (Malo and Worcester, 1975; Miller et al., 1988; Stone et al., 1985). Another feature of the output maps is the excluded regions (shown in white) where photo-

tone values (of at least one image band) are not within the range of data extracted from the images for analysis. Regression models would have to be extrapolated to obtain predictions in these regions, which would be statistically invalid.

## Summary of Soil-Water-Monitoring Data

Soil water data collected during the 1992 growing season showed distinct patterns of soil-water storage (monitoring locations are shown in Figure 2). The wettest soils occurred in upland subsoils, and are associated with depositional and illuvial (lamellae) layering in fine sands. The driest conditions occurred in alluvial subsoils at lowland positions (Figures 6a and 6b). Surface soils are driest at upland and backslope positions (Figure 6b), where ranges of profile water storage were least (Figure 6c). This suggests that the lesser yield and N uptake at backslope and upland positions is caused by lower water availability. A detailed study of soil water storage across an adjacent hillslope is described by Tomer and Anderson (1995).

During two periods of water depletion, the toeslope positions showed the greatest rates of water loss (Figure 6d). This suggests one of two situations: (1) evapotranspiration was uniform along the transect during these two periods, and percolation losses were greatest at the toeslope positions; or (2) percolation losses were minimal during crop growth; therefore, evapotranspiration was not uniform along the transect, and water availability or rooting patterns allowed more efficient water use at the toeslope positions. The second con-



Estimated Corn Yield, 1991:

Estimated Nitrogen Uptake, 1991:

Legend (kg/ha):

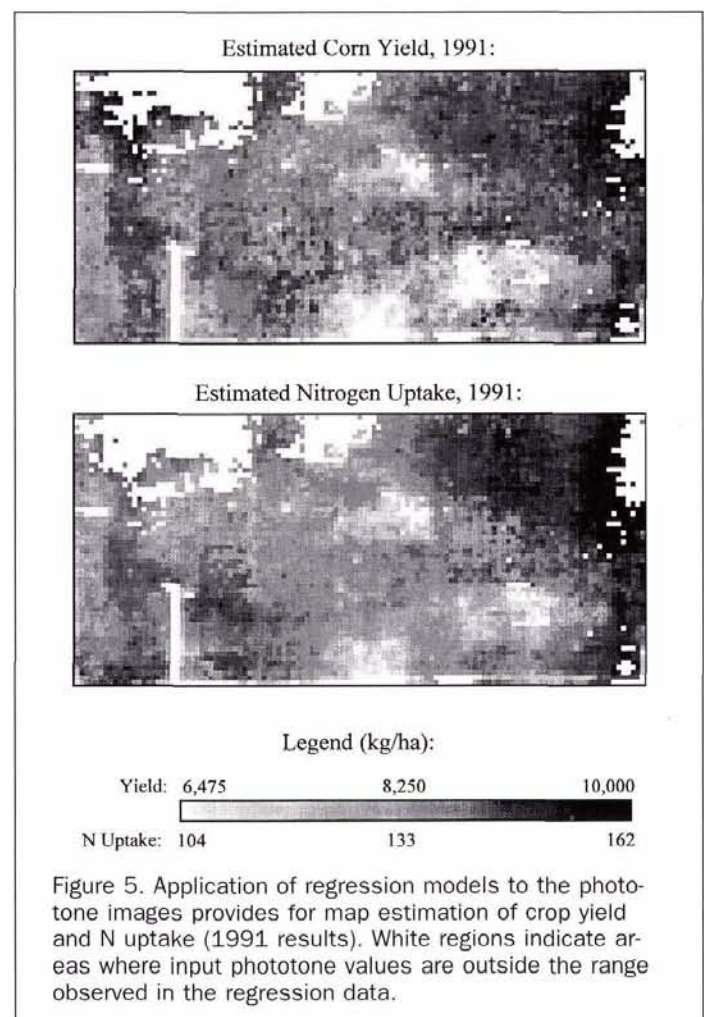| Yield: 6,475 | 8,250 | 10,000 |
| N Uptake: 104 | 133 | 162 |

Figure 5. Application of regression models to the phototone images provides for map estimation of crop yield and N uptake (1991 results). White regions indicate areas where input phototone values are outside the range observed in the regression data.
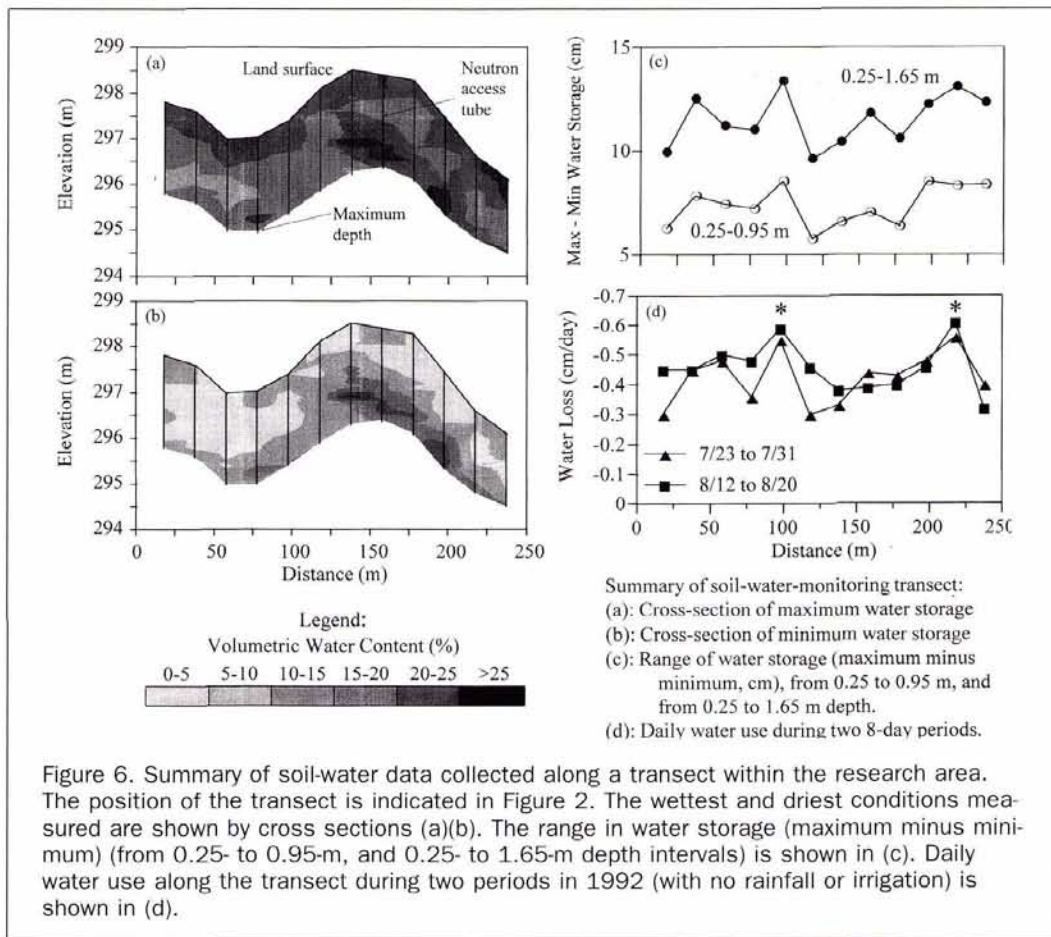
Figure 6. Summary of soil-water data collected along a transect within the research area. The position of the transect is indicated in Figure 2. The wettest and driest conditions measured are shown by cross sections (a)(b). The range in water storage (maximum minus minimum) (from 0.25- to 0.95-m, and 0.25- to 1.65-m depth intervals) is shown in (c). Daily water use along the transect during two periods in 1992 (with no rainfall or irrigation) is shown in (d).

clusion is consistent with observed corn yield and N uptake patterns, which were greatest at toeslope positions.

## Summary and Conclusions

Photometric indicators of relative red and infrared reflectance from physiologically mature crop, and of relative infrared reflectance from bare soil, were consistently significant in predicting yield and N uptake across a two-year study. Therefore, data from scanned infrared photographs can be used to predict variation of corn grain yield and N uptake on this sandy landscape. This method had better predictive capacity than use of topographic data or geostatistical methods. This success of the method must be tempered because the predictive capacity is affected by climatic differences from year to year. Climatic conditions that allow soil conditions to be manifested in crop growth patterns optimize results of these photographic mapping techniques. These conditions include sufficient heat, radiation, and precipitation to meet crop needs (a "normal" growing season), and limited water stress to cause differentiation in the crop as it matures.

Although spatial modeling of crop growth with aerial photographs is possible, multi-year and multi-site studies will be necessary to further develop and fully document the utility of these techniques. Such an effort could lead to an operational mapping method for site-specific management, and to a better understanding of landscape effects on crop growth patterns. If this effort is undertaken, the issue of cause and effect must also be addressed. In this study, consistencies were found between crop-growth and water-storage patterns. Landscape variations observed through spatial modeling must be related to soil conditions, or else may apply poorly to soil-specific management.

## References

Baber, J.J., 1982. Detecting crop conditions with low altitude aerial photography: Causes and effects, non uniformity of fertilizer application, poor water pattern, drainage needs, *Remote Sensing for Resource Management* (C.J. Johannsen and J.L. Sanders, editors), Soil Conserv. Soc. Am., Ankeny, Iowa, pp. 407–412.

Campbell, J.B., 1987. *Introduction to Remote Sensing*, Guilford Press, New York, 551 p.

Collins, W., 1978. Remote sensing of crop type and maturity, *Photogrammetric Engineering & Remote Sensing*, 44:43–55.

Colwell, J.E., 1974. Vegetation canopy reflectance, *Remote Sens. Env.*, 3:175–183.

ERDAS, 1991. *ERDAS Field Guide, Second Edition, Ver. 7.5*, ERDAS, Inc., Atlanta, Georgia, 394 p.

Delin, G.N., M.K. Landon, J.A. Lamb, and J.L. Anderson, 1994. *Characterization of the Hydrogeology and Water Quality at the Management System Evaluation Area near Princeton, Minnesota, 1991-92*, U.S. Geol. Surv. Water Res. Invest. Rpt. 94-4194, 54 p.

ESRI, 1992. *ARC/INFO User's Guide: ARC Command References, Ver. 6.1*, Env. Sys. Research Inst., Inc., Redlands, California.

Everitt, J.H., D.E Escobar, M.A. Alaniz, and M.A. Hussey, 1987. Drought-stress detection of buffelgrass with color-infrared aerial photography and computer-aided image processing, *Photogrammetric Engineering & Remote Sensing*, 53:1255–1258.

Frazier, B.E., and Y. Cheng, 1989. Remote sensing of soils in the eastern Palouse region with landsat thematic mapper data, *Remote Sens. Env.*, 28:317–325.

Freund, R.J., and R.C. Littell, 1991. *SAS System for Regression, Second Edition* (second printing), The SAS Institute, Cary, North Carolina, 210 p.

Gerten, D.M., and M.V. Wiese, 1987. Microcomputer-assisted video image analysis of lodging in winter wheat, *Photogrammetric Engineering & Remote Sensing*, 53:83–88.

Griffith, D.A., and C.G. Amrhein, 1991. *Statistical Analysis for Geographers*, Prentice-Hall, Inc., Englewood Cliffs, New Jersey, 478 p.

Haan, C.T., 1986. *Statistical Methods in Hydrology* (4th printing), Iowa St. Univ. Press, Ames, Iowa, 378 p.

Harrison, W.D., M.E. Johnson, and P.F. Biggam, 1987. Video Image Analysis of Large Scale Vertical Aerial Photography to Facilitate Soil Mapping, *Soil Survey Techniques* (W.U. Reybdd and G.W. Peterson, editors), Soil Sci. Soc. Am. Spec. Pub. 20, ASA-CSSA-SSSA, Madison, Wisconsin, pp. 1–9.

Henderson, T.L., A. Szilagyi, M.F. Baumgardner, C.T. Chen, and D.A. Landgrebe, 1989. Spectral band selection for classification of soil organic matter, *Soil Sci. Soc. Am. J.*, 53:1774–1778.

Kunze, B.O., and G.D. Lemme, 1986. Photography for order 2 soil surveys, *Soil Surv. Hor.*, 27:10–17.

KHOROS, 1991. *KHOROS User's Manual, Vol. 1, Rel. 1*, Univ. of New Mexico.

Long, D.S., G.A. Nielson, and G.R. Carlson, 1989. Use of aerial photographs for improving layout of field research plots, *Appl. Agric. Res.*, 4:96–100.

Lyon, J.G., J.F. McCarthy, and J.T. Heinen, 1986. Video digitization of aerial photographs for measurement of wind erosion damage on converted rangeland, *Photogrammetric Engineering & Remote Sensing*, 52:373–377.

LMIC, 1990. *EPPL7: Environmental Planning and Programming Language. Ver. 7.0, Users Guide, Rel. 2.0*, Minnesota State Planning Agency, Land Management Information Center, St. Paul, Minnesota, 126 p.

Malo, D.D., and B.K. Worcester, 1975. Soil fertility and crop responses at selected landscape positions, *Agron. J.*, 67:397–401.

Microsoft, 1992. *Microsoft Excel Users Guide, Ver. 4.0*, Microsoft Corp., Redmond, Washington.

Milfred, C.J., and R.W. Kiefer, 1976. Analysis of soil variability with repetitive aerial photography, *Soil Sci. Soc. Am. J.*, 40:553–557.

Miller, M.P., M.J. Singer, and D.R. Nielsen, 1988. Spatial variability of wheat yield and soil properties on complex hills, *Soil Sci Soc. Am. J.*, 52:1133–1141.

Nelson, D.W., and L.E. Sommers, 1973. Determination of total nitrogen in plant materials, *Agron. J.*, 65:109–112.

SAS Institute, 1988. *SAS/STAT User's Guide, Rel. 6.03 Edition*, SAS Institute, Inc., Cary, North Carolina, 1028 p.

Sawyer, J.E., 1994. Concepts of variable-rate technology with considerations for fertilizer technology, *J. Production Agric.*, 7:195–201.

Schmidt, R., B. Thamm, and A. Richter, 1987. Interpretation of aerial photographs for describing the composition of the soil mantle in ground moraine regions, *Arkiv für Acker und Pflanzenbau und Bokenkunde*, 31:71–79.

Soil Survey Staff, 1992. *Keys to Soil Taxonomy, 5th Edition*, SMSS Technical Monograph No. 19, Pocahontus Press, Inc., Blacksburg, Virginia, 556 p.

Stone, J.R., J.W. Gilliam, D.K. Cassel, R.B. Daniels, L.A. Nelson, and H.J. Kliess, 1985. Effect of erosion and landscape position on the productivity of Piedmont soils, *Soil Sci. Soc. Am. J.*, 49:987–991.

Stoner, E.R., and M.F. Baumgardner, 1981. Characteristic variations in reflectance of surface soils, *Soil Sci. Soc. Am. J.*, 45:1161–1165.

Stephens, P.R., J.K. MacMillan, J.L. Daigle, and J. Cihlar, 1985. Estimating universal soil loss equation values with aerial photography, *J. Soil Water Cons.*, 40:293–296.

Tomer, M.D., and J.L. Anderson, 1995. Variation of soil-water storage across a sand-plain hillslope, *Soil Sci. Soc. Am. J.*, 59:1091–1100.

Tucker, C.T., 1979. Red and photographic infrared linear combinations for monitoring vegetation, *Remote Sens. Env.*, 8:127–150.

Webster, R., and M.A. Oliver, 1990. *Statistical Methods in Soil and Land Resource Survey*, Oxford Univ. Press, New York, 316 p.

Zheng, F., and H. Schreier, 1988. Quantification of soil patterns and field soil fertility using spectral reflection and digital processing of aerial photographs, *Fertilizer Res.*, 16:15–30.

## Appendix

The following statistical brief is provided to introduce terms:

Principle components analysis (PCA) is used to eliminate redundancy within a data set. In essence, PCA reorients the coordinate system of a multivariate data set according to the attributes of the data. For example, the centroid of the data becomes the origin of the new coordinate system, and the primary axis (first PC) is oriented (by a linear combination of the original variates) to capture the greatest possible variance of the data. Succeeding axes (or components) are orthogonal and account for successively less variation in the original data set. The number of components is always equal to the number of original variates. Haan (1986) and Webster and Oliver (1990) provide primers on PC analysis with examples.

Spatial data often exhibit spatial autocorrelation. When measurements are made in space, there is an expectation that two measurements made close together will be more similar to one another than will a pair of measurements made far apart. A spatial data set that follows this expectation is said to be autocorrelated. Most methods of interpolation rely on this principal. The variogram and the correlogram are two (essentially equivalent) methods of measuring the degree and spatial length of autocorrelation. The variogram is a plot of variances of differences between paired measurements ($\gamma$, plotted on the $Y$ axis) versus distance between the paired observations ($h$). In practice, data pairs are grouped into classes of increasing separation distances, and $\gamma$ is estimated for the modal separation ($h$) within each class to give a single point on the variogram. The equation for $\gamma(h)$,

$$\gamma(h) = \sigma^2(X) - \text{Cov}(X_i, X_{i+h}), \qquad (A1)$$

is obtained directly from the general formula describing the variance of a difference between two variables (see Webster and Oliver, 1990). The correlogram is obtained directly from Equation A1 by scaling the variogram by the population variance,

$$\rho(h) = 1 - \gamma(h)/\sigma^2. \qquad (A2)$$

In this equation, $\rho(h)$ is the autocorrelation parameter (for separation vector $h$), which has an expected value near zero as paired measurements become uncorrelated.

Kriging is a method of interpolation that is based on a model fit to the variogram. Some common variogram models are linear, spherical, and exponential (see Webster and Oliver, 1990). Kriging errors are estimated by a jackknifing procedure, in which each observation is removed and then estimated from the surrounding data points. The observed minus the estimated value gives the kriging error. Further discussions on spatial analysis and interpolation are given by Webster and Oliver (1990) and Griffith and Amrhein (1991).

Our methods also included techniques of multivariate regression, including selection, and evaluation of regression models. For overview and discussion of these issues, refer to Freund and Littell (1991), Haan (1986), and Webster and Oliver (1990).